Fabrication of Porous Co_3O_4 Arrays by a Co-Precipitation Method and it Application as a Non-Enzymatic Glucose Sensor

[1]Jie Zhang, [2]Ri Xia, [1]Xianchun Li* and [2]Jiasheng Xu**

[1]*School of Chemical Engineering, University of Science and Technology Liaoning, Anshan 114051, P.R. China.*
[2]*College of Chemistry, Chemical Engineering and Environmental Engineering, Liaoning Shihua University, Fushun, 113001, P.R. China.*
*xianchunli@ustl.edu.cn; **jiashengxu@lnpu.edu.cn

Summary: The porous cobaltosic oxide (Co_3O_4) arrays has been prepared by a chemical co-precipitation route using the nickel foam as s substrate. Cyclic voltammetry (CV), and ampere current method (i-t curve) are used to explore the non-enzymatic glucose sensor in a three-electrode system. This porous Co_3O_4 array non-enzymatic sensor shows a sensitivity of 592.8 mA mM^{-1} cm^{-2} in concentration from 0.99 μM to 1.073 mM. The porous Co_3O_4 array sensor electrode also showed low LOD value (0.005 μM) and fast response time (4 s). This porous Co_3O_4 electrode shows a good sensor performance due to these rich redox reaction sites in the unique porous structure. This porous cobaltosic oxide arrays maybe a potential sensor material in the glucose detection application.

Introduction

With modern medical diagnostic techniques for the glucose measurement standard increasing, glucose detection technology has attracted more and more attentions [1-4]. Notwithstanding various types of glucose detection technologies as electronic, optical, acoustic, electromagnetism, thermal are researched [5-9]. The high sensitive non-enzyme electrochemical glucose detection sensor electrode materials are the key contents of this research field [10]. Glucose biosensors are usually divided into enzyme type and non-enzyme type. Since 1980, enzymatic glucose sensors have been widely used and successfully commercialized. However, in the process of using enzyme sensor, the biological enzyme of sensitive element has many disadvantages. The biggest disadvantage of enzyme glucose sensor is poor stability and high maintenance cost. The biological enzyme itself is very sensitive to the external environment [11, 12]. Recently, many researchers are beginning to pay attention to non-enzymatic glucose sensor electrode materials [13, 14].

Due to more advantages, the non-enzymatic electrochemical glucose sensors have been widely studied recently [15-17]. The transition metal oxides can be used to prepare non-enzyme glucose sensor electrode materials. Moreover, the price of these metal oxides is relatively low, the raw materials are easy to obtain, it can provide appropriate overpotential with glucose molecules to produce fast and sensitive chemical reaction signals [18-23]. Cobalt trioxide (Co_3O_4) is the spinel structure (AB_2O_4). Co_3O_4 belongs to the AB_2O_4 crystal structure, and its molecular formula can be regarded as $CoCo_2O_4$. In the electrocatalytic redox reaction, CO^{3+}/Co^{4+} redox pairs can be produced by CO^{3+}/Co^{4+}. In addition, Co_3O_4 also provides high electroactivity, low cost, environmental friendliness and relatively good conductivity [24, 25]. Therefore, the development of nanostructured Co_3O_4 electrode as material has a great significance for the glucose detection [13, 26]. For example,

In this work, porous Co_3O_4 array sensor electrodes have been prepared by room temperature co-deposition and heat treatment. The porous cobaltosic oxide arrays has been prepared by a chemical co-precipitation route using the nickel foam as s substrate. The commercial nickel foam is low cost, high conductivity and abundant pore structure. It provides unique microstructure for directly growing porous Co_3O_4 array structure.

Experimental

Preparation of porous Co_3O_4 array on foam nickel sensor electrode

The nickel foam can been firstly washed in an ultrasonic cleaning tank for 30 minutes with 2 M

---

*To whom all correspondence should be addressed.

hydrochloric acid to remove oxide impurity layer. Then foam nickel is cleaned with ethanol and a large amount of deionized water. The Co_3O_4 array foam nickel sensor electrode is prepared by chemical co-deposition method. In this reaction, the oxalic acid ($H_2C_2O_4 \cdot 2H_2O$) was used as the precipitator. The cobalt nitrate solution (0.1 M) was added into this oxalic acid solution (0.1 M, with the pretreated nickel foam), and the molar ratio of oxalic acid and cobaltous nitrate is 2, maintained stirring for 30 minutes. Then, the nickel foam was collected and washed thoroughly and dried for 2 hours. Finally, the nickel foam precursor was heat-treated for 2 hours at 350 °C and cooled to ambient temperature. The porous Co_3O_4 array non-enzyme glucose sensor electrode was obtained.

Instruments and characterizations

X-ray diffraction (XRD) measurement was carried out using the Rigaku RAD-3C diffractometer instrument (Cu Kα, λ=1.5405 Å, 35 kV, 20 mA, *2-Theta* angles: 10°–70°). The morphology and structure were investigated by scanning electron microscopy (SEM, JEOL S-4800) under the condition of 3.0 kV operating voltage. Transmission electron microscopy (TEM, JEOL JEM-2100F microscopy) was also carried out to investigate the element distributions of porous Co_3O_4 array under the condition of 200 kV accelerating voltage. X-ray photoelectron spectroscopy (XPS, ESCALB-MKII250) was performed to analyze the elemental compositions and its valence of porous Co_3O_4 array under a monochromatic 150 W Al Kα source radiation. Nitrogen adsorption/desorption measurement was performed to analyze the specific surface area of porous Co_3O_4 array on a Micromeritics ASAP 2010 analyzer at 77 K.

Porous Co_3O_4 array on foam nickel electrode for glucose detection

The performance of the porous Co_3O_4 array on foam nickel electrode is investagated in the electrochemical workstation of CHI 660D made in China. The three-electrode system is used in glucose detection process. The porous Co_3O_4 array on foam nickel electrode is used as the working electrode, the platinum (Pt) electrode as the counter electrode, the Hg/HgO electrode as the reference electrode in a 0.5 M sodium hydroxide solution. By using cyclic voltammetry (CV), ampere current method (i-t curve) and electrochemical impedance spectroscopy (EIS) method, the electrochemical performance of the

porous Co_3O_4 array on foam nickel electrode sensor was investegated under the experimental ambient temperature of 25 °C. Cyclic voltammetry and amperometric method were used to test glucose under magnetic stirring at 400 revolutions per minute, and EIS test was carried out without stirring.

Results and Discussion

XRD diffraction pattern of porous Co_3O_4 array material is shown in Fig. 1a. These peaks at 30.1°, 35.4°, 37.0°, 43.0°, 53.2°, 56.9°, 62.5° and 73.9° correspond to (220), (311), (222), (400), (422), (511), (440) and (533) crystal plane standard diffraction patterns of spinel (AB_2O_4) cobalt trioxide (Co_3O_4) phase (JCPDS No. 43–1003, $a = b = c = 8.08$ Å, space group: cube *Fd-3m*(227), Z=8)[27]. It further shows the high purity of the porous Co_3O_4. The peaks with wide width and weak intensity show that the porous Co_3O_4 array has low crystallinity [28]. In the following SEM and TEM images, the Co_3O_4 material synthesized in this work is polycrystalline and porous. These structural characteristics can improve their electrochemical properties, because many loosely stacked nano materials can improve the application performance of their sensors [29]. Fig. 1b is a typical BET test isotherm of porous Co_3O_4 array electrode. The nitrogen desorption adsorption test isotherm was drawn by taking the volume (V_m) and the relative pressure (P/P_0). The BET specific surface area of porous Co_3O_4 array is 49.1 m^2 g^{-1}. The isotherm of nitrogen desorption and adsorption test shows hysteresis. According to the distribution of hysteresis loop, it is the type III isotherm with H3 hysteresis loop. Fig. 1b Inset shows the average pore size (7.8 nm). The spectrum of the cobalt element (Fig. 1c) shows two typical peaks for cobalt regions centered at 779.9 eV and 794.9 eV, corresponding to Co 2p 3/2 and Co 2p 1/2 of Co^{3+}, respectively. The typical peak at 781.5 eV corresponding to Co 2p 3/2 of Co^{2+}, respectively. Two prominent satellite peaks of Co 2p 3/2 and Co 2p 1/2 were observed at 789.9 eV and 804.7 eV, respectively. A binding energy separation of 15 eV, which is in good agreement with the Co 2p 3/2 and Co 2p 1/2 energy level in Co_3O_4. These results indicated the successful fabrication of porous Co_3O_4 array. The spectrum of the oxygen element (Fig. 1d) displays two peaks at binding energy of 529.8 eV and 531.9 eV are observed, which corresponding to the characteristic bands of the metal-oxygen bonds in Co_3O_4 and metal surface hydroxyl groups, respectively.
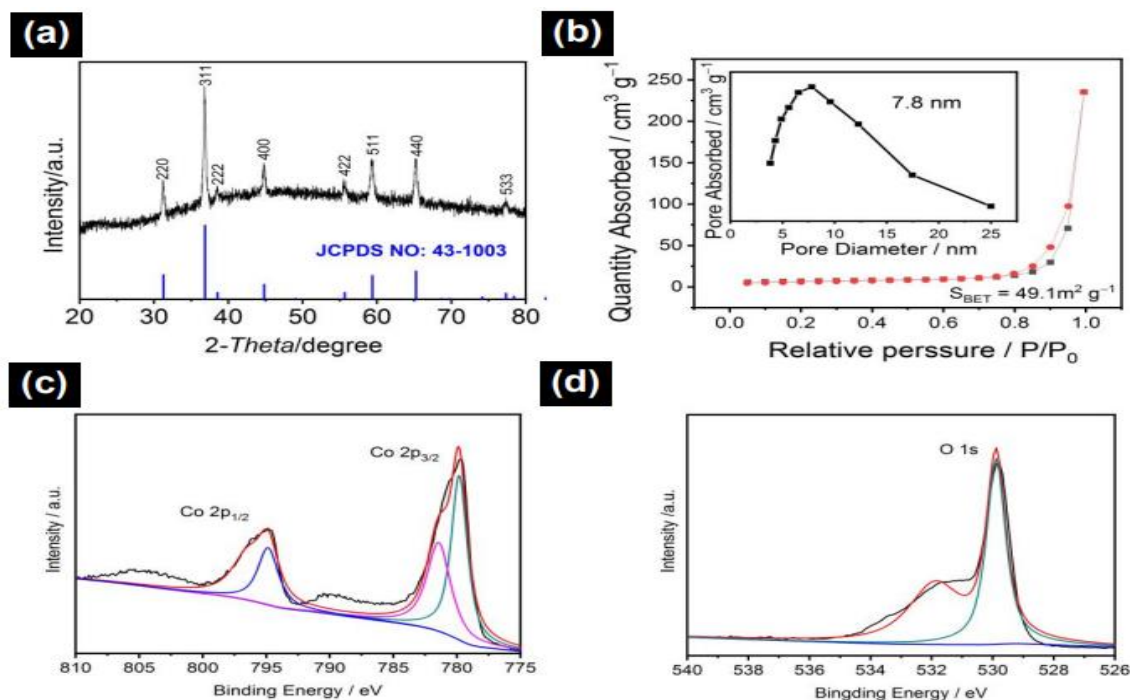
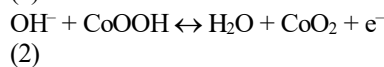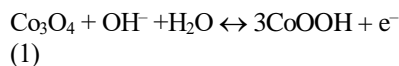Fig. 1:   (a) XRD patterns of porous Co_3O_4 arrays sensor electrode. The standard diffraction pattern of Co_3O_4 (JCPDS NO 43-1003) is shown as a reference. (b) BET nitrogen adsorption and desorption isotherms of porous Co_3O_4 arrays sensor electrode, Inset is the pore size distribution plot with based on BJH measurement. (c) XPS spectra of Co 2p spectrum and (d) O 1s spectrum.

Fig. 2a is a SEM image at a lower magnification. From the SEM images at low magnification, the porous Co_3O_4 were evenly and completely covered on the surface of the foam nickel substrate. Porous Co_3O_4 in the foamed nickel substrates form three dimensional ordered porous Co_3O_4 arrays. Fig. 2b shows SEM images of porous Co_3O_4 array electrodes at medium magnification. The length of porous Co_3O_4 is about 5 μm and the width of porous Co_3O_4 is about 600 nm. Fig. 2c shows the SEM image of porous Co_3O_4 array electrode with high magnification, and the porous structure of the surface can be clearly seen. The porous structure further forms a three-dimensional spatial structure. This unique structure can shorten the diffusion / transmission distance. The porous Co_3O_4 array provides a larger surface area for electrocatalytic reaction. Fig. 2e is the overall contour of Co_3O_4, which is the porous structure, and the width is 600 nm. The lattice stripes with crystal plane spacing of 2.858 and 2.437 Å can be clearly seen, which correspond to (220) and (311) crystal planes of Co_3O_4 phase (Fig. 2f). The lattice fringes consist with XRD diffraction patterns. The SAED pattern consists of two light diffraction rings (Fig. 2g). The diffraction ring matches the (220) and (311) crystal surfaces of the porous Co_3O_4 respectively, indicating the existence of the porous Co_3O_4 and its polycrystalline structure[30].

The porous Co_3O_4 array electrode was directly used in the glucose sensor. Fig. 3a is the CV curves of Co_3O_4 array (10 – 100 mV s^{-1}). The electrolyte solution is 0.5 M NaOH. These peaks are the electrochemical redox reaction of porous Co_3O_4 array electrode during glucose detection. The reaction equations are as follows (1), (2) and (3) [31].

$$Co_3O_4 + OH^- + H_2O \leftrightarrow 3CoOOH + e^-$$
(1)
$$OH^- + CoOOH \leftrightarrow H_2O + CoO_2 + e^-$$
(2)
$$2CoO_2 + glucose \rightarrow 2CoOOH + gluconolactone \quad (3)$$

As shown in Fig. 3a, in the deferent scanning rates, the corresponding pairs of redox peaks are observed. Fig. 3b is the fitting curve of the peak current to the square root of the scanning rate. These peaks increase linearly with the scanning rate, which means the ion transfer is reversible [32]. Fig. 3c shows the CV curves in the deferent glucose concentrations (0, 1, 2, 3, 4, 5, 6, 7 and 8 mM). From the CV curve of porous Co_3O_4 array sensor electrode (Fig. 3d), the peak of redox reaction increases steadily, and there is almost no change in shape. These results show that porous Co_3O_4 array electrode has good electrochemical sensing performance for glucose.
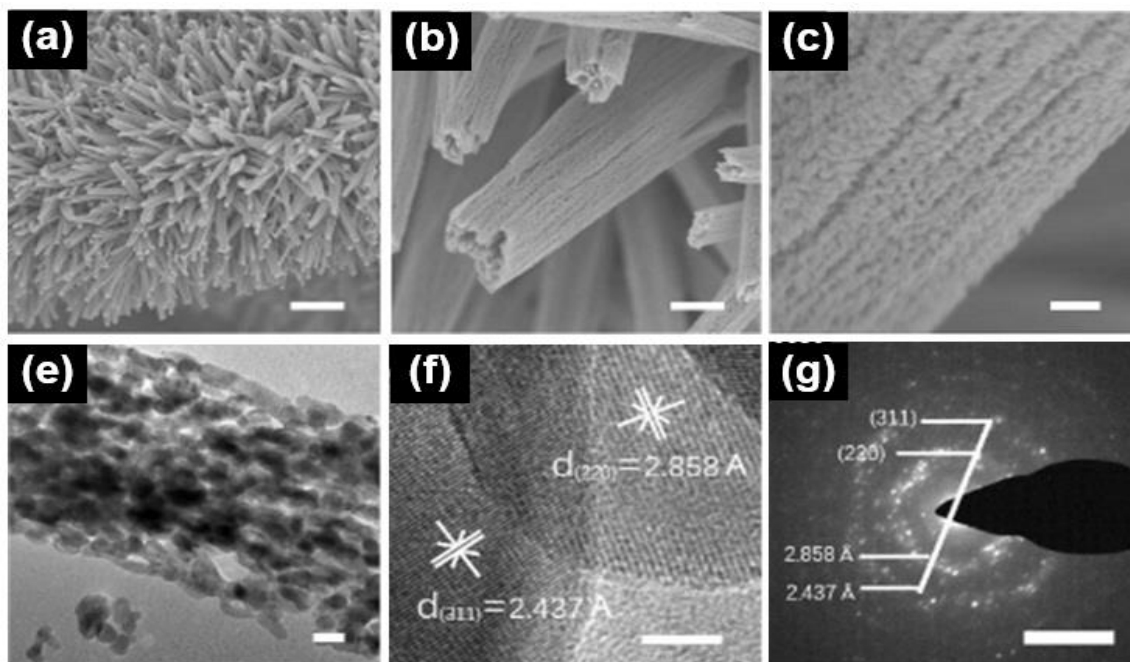
Fig. 2:   (a) Low magnification SEM image of porous Co_3O_4 sensor electrode, scale bar = 5 μm. (b) Medium magnification SEM images, scale bars = 500 nm. (c) High magnification SEM image, scale bar = 100 nm. (e) Low magnification TEM image, scale bar = 50 nm; (f) High resolution TEM (HRTEM) images, scale bar = 5 nm; (g) Selected area electron diffraction (SAED) patterns, scale bar = 5 1/nm

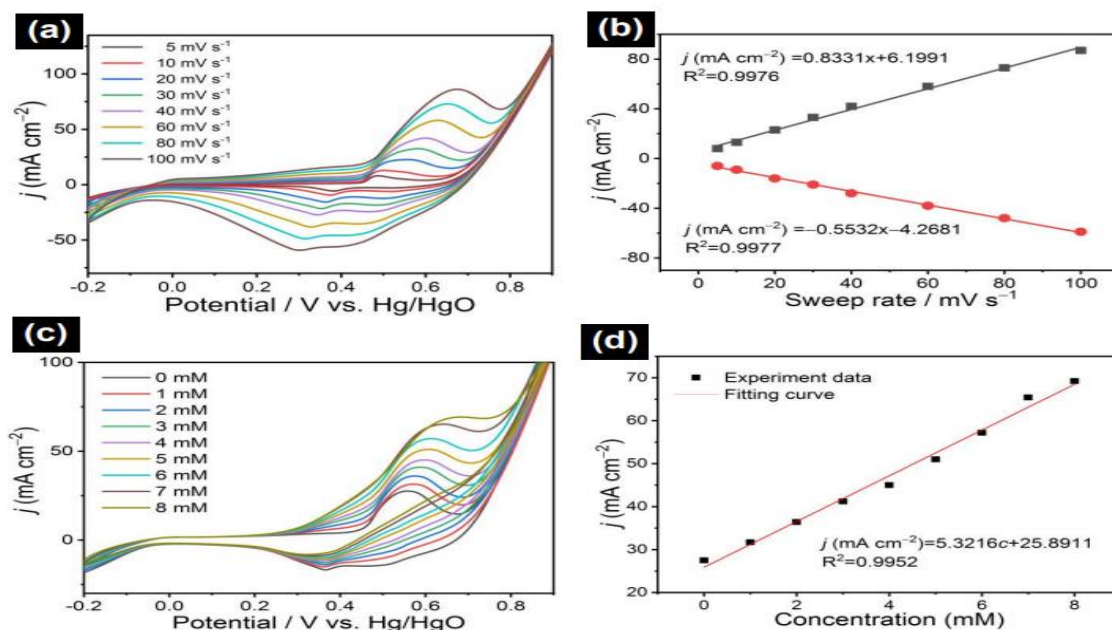Fig. 3:   (a) CV curves of porous Co_3O_4 sensor electrode in 0.5 M NaOH electrolyte. (b) The corresponding fitting curves of anode and cathode peak response currents for (a) as a function of the square root of sweep rates. (c) CV curves of porous Co_3O_4. (d) The corresponding fitting curves of anode and cathode peak response currents for (c) as a function of the square root of sweep rates.
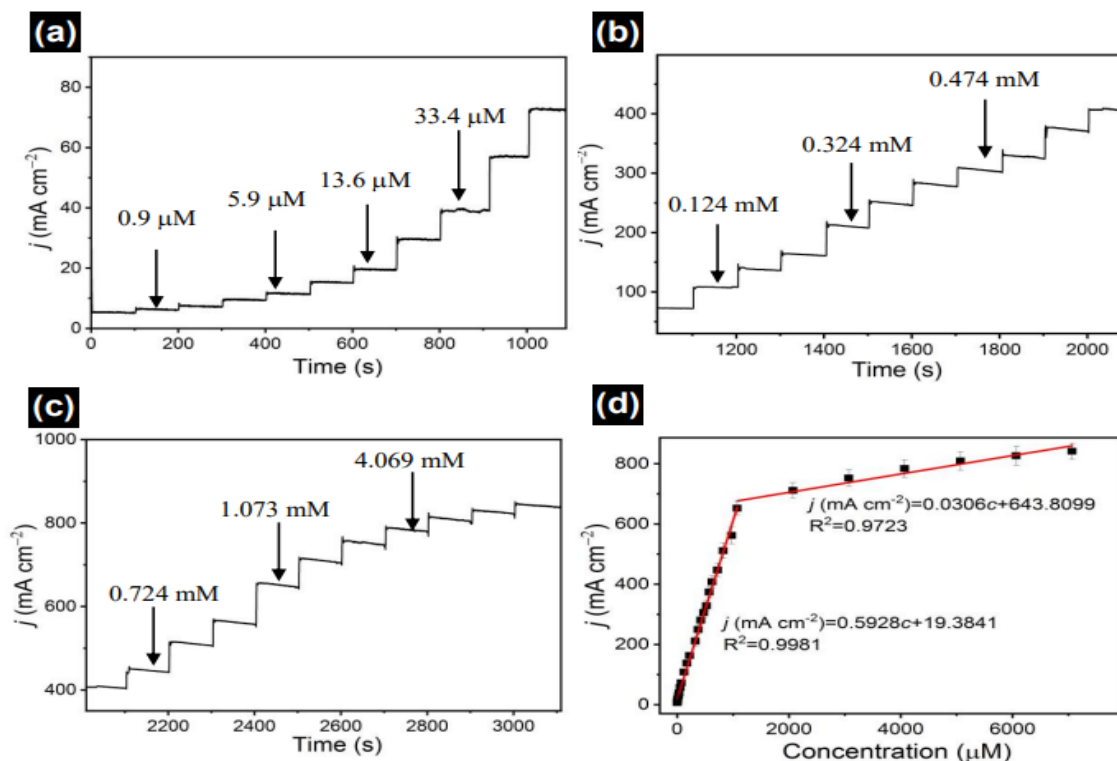
Fig. 4:   The amperometric responses of porous Co_3O_4 arrays on nickel foam sensor with various concentration glucose. (a) The amperometric responses of low concentration for glucose; (b) The amperometric responses of medium concentration for glucose; (c) The amperometric responses of high concentration for glucose; (d) The corresponding fitting curves at different concentrations.

The electrochemical response characteristics of porous Co_3O_4 array sensor electrode can be tested by ampere current method. In this electrochemical detection system, the response time was tested at a potential of +0.45V. The current time gradient curve of porous Co_3O_4 array sensor electrode in the low concentration range of 0.9–74.1 μM is shown in Fig. 4a. When glucose solution is added to NaOH electrolyte solution, different current responses can be clearly observed in the electrolytic cell, which shows that the porous Co_3O_4 array sensor electrode has good current response characteristics in glucose detection. Fig. 4b shows the current time gradient curve from 74.1 μM–0.625 mM. With the increasing concentration of glucose solution, the porous Co_3O_4 array sensor electrode always conducts electrons rapidly. Fig. 4c shows the current time gradient curve of porous Co_3O_4 array sensor from 0.625 mM to 7.067 mM.

Fig. 4d shows the corresponding fitting curves of porous Co_3O_4 array sensor electrodes in two different concentration ranges (0.99 μM–1.073 mM and 1.073 mM–7.067 mM). The regression equations

corresponding to the fitting curve are: j(mA cm^{-2}) = $0.5928c$ (μM)+19.3841 (R^2 = 0.9981) and j(mA cm^{-2})= $0.0306c$ (μM) + 643.8099 (R^2 = 0.9723). According to the fitting curve, the detection sensitivity of porous Co_3O_4 array sensor electrode is 592.8 mA mM^{-1} cm^{-2} (in the concentration from 0.99 μM to 1.073 mM), and the detection sensitivity of porous Co_3O_4 array sensor electrode is 30.6 mA mM^{-1} cm^{-2} (from 1.073 mM to 7.067 mM). Porous Co_3O_4 array sensor electrode shows good sensitivity at low concentration. As can be seen from Fig. 4d, these current responses increase with the glucose concentration. This detection limit (LOD) of porous Co_3O_4 array sensor electrode is calculated using the following formula (4)[33].

$$LOD = 3SD/S \quad (4)$$

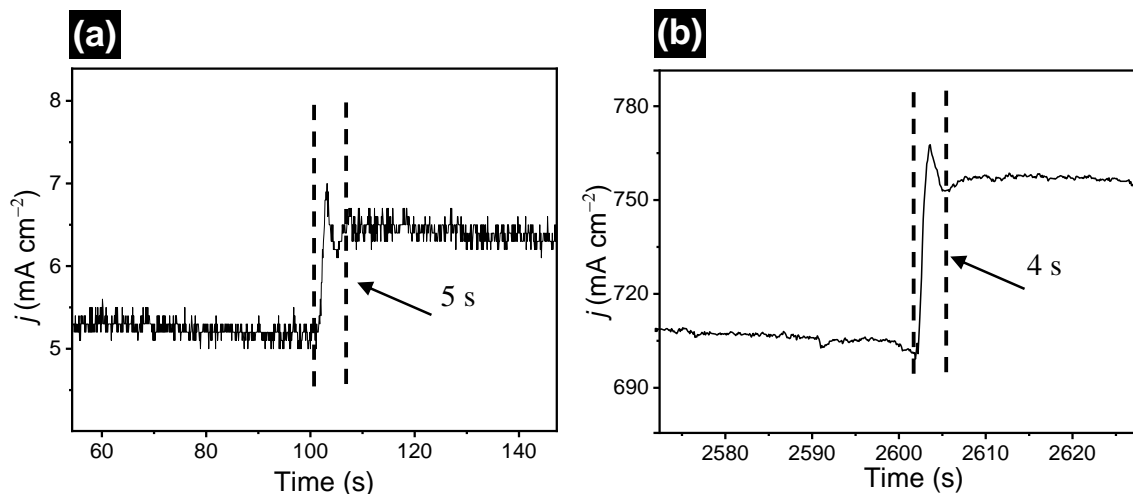Here S is 0.5928 mA μM^{-1} cm^{-2}, SD is 9.9×10^{-4} mA cm^{-2}. The LOD is 0.005 μM.

Fig. 5:   The response time of porous Co_3O_4 sensor electrode (a) A response time of 5 s at a gluconic concentration of 0.9 μM; (b) A response time of 4 s at a gluconic concentration of 3.070 mM.

Table-1: Comparison of the electrochemical performance of glucose detection for the porous Co_3O_4 arrays on nickel foam sensor in this work and the previously reported transition metal based sensors.

Materials	Sensitivity mA mM^{-1} cm^{-2}	Linear range μM	LOD μM	Response time s	References
Co_3O_4/nanoporous gold	4.47	2–2110	0.085	2	[35]
Co_3O_4 nanoclusters	1.38	88–7700	26	-	[36]
Co_3O_4-NiO nano-needles	0.062	1–3400	0.81	-	[37]
S-doped Co_3O_4 shell	1.27	0.2–3100	0.09	-	[38]
Co_3O_4/CuO nanorod	5.41	1–500	0.38	2	[39]
Cu-doped Co_3O_4 film	1.85	18.3–1440	0.153	10	[40]
Co_3O_4-N-doped carbon	2.56	0.5-20	0.05	-	[41]
Co_3O_4 acicular nanotube	2.0	200–1000	0.3396	5	[42]
Co_3O_4 nanofibers	0.014	100−8000	60	6	[43]
Co_3O_4-CeO_2 nanosheets	0.019	5–1500	0.21	-	[44]
Co_3O_4/ carbon nanotube	2.55	1–122	0.28	14	[45]
Co_3O_4 needles/Au honeycomb	2.01	20–4000	20	120	[46]
Co_3O_4/carbon cloth	0.246	0.5–1000	0.012	-	[47]
porous Co_3O_4 arrays	592.8 30.6	0.99–1073 1073–7067	0.005	4	In this work

Test response time is a key parameter of electrochemical sensor. This response time of porous Co_3O_4 array sensor was obtained by current time test. Fig. 5 shows the response time of porous Co_3O_4 array sensor electrode. By adding glucose to the electrolyte solution, glucose oxidizes to generate electrons, resulting in a rapid increase in current and then reaching a stable state. Fig. 5a shows the response time of porous Co_3O_4 array sensor electrode is 5 seconds (the concentration is 0.9 μM). Fig. 5b shows that the response time of the porous Co_3O_4 array sensor electrode is 4 seconds at a glucose concentration of 3.070 mM. The results show that the porous Co_3O_4 array sensor electrode has fast ampere current response time and good sensitivity. The comparison for the sensing performances of porous Co_3O_4 array and other transition metal oxide materials is listed as shown in Table-1. This comparison table shows the excellent sensing performances of porous Co_3O_4 array electrode compared to the reported sensor.

The anti-interference (selectivity) of porous Co_3O_4 array is very important for glucose detection. As shown in Fig. 6, the ampere current responses of Citric Acid, Urea, Ascorbic Acid and NaCl were tested in the same NaOH electrolyte. By adding 1.0 mM glucose, Citric Acid (CA), Urea, Ascorbic Acid (AA), NaCl into the electrolyte, a significant response current is at 200 s and 900 s, which are the response of the glucose. The current response generated by these interfering substances (CA, Urea, AA, and NaCl) can be negligible[34]. The selectivity of the porous Co_3O_4 array sensor electrode is good. Therefore, the anti-interference (selectivity) test results of porous Co_3O_4 array sensor electrode show that porous Co_3O_4 array sensor will have good potential in practical application in the non-enzymatic glucose detection.
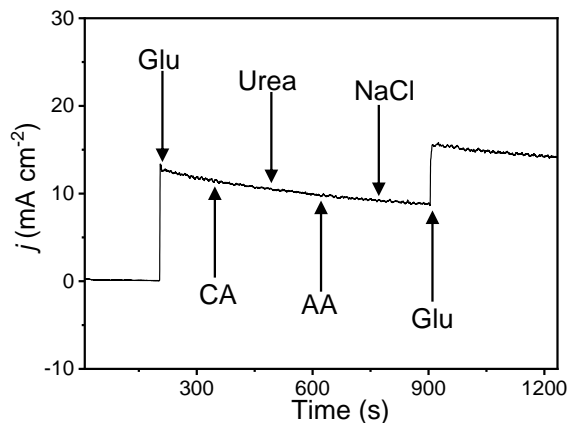
Fig. 6:   Selectivity of porous Co_3O_4 arrays on nickel foam sensor.

Conclusion

The porous Co_3O_4 array electrodes have been successfully prepared by coprecipitation reaction and heat treatment. The porous Co_3O_4 array sensor electrode has been investigated in the electrochemical sensor test. This unique porous Co_3O_4 array provides more electrocatalytic active sites, to promote rapid electron ion transfer efficiency. The porous Co_3O_4 array sensor electrode has good performance, with good selectivity, stability, high sensitivity, reversible and rapid response. The porous Co_3O_4 array sensor electrode showed a high sensitivity of 592.8 mA mM^{-1} cm^{-2} in the concentration from 0.99 μM to 1.073 mM. The porous Co_3O_4 array sensor electrode also showed low LOD value (0.005 μM) and fast response time (4 s). These good electrochemical detection properties of glucose show that porous Co_3O_4 array sensor electrode has good potential and practical application prospect as non-enzymatic sensing materials.

References

1. R. Batool, A. Rhouati, M. H. Nawaz, A. Hayat and J. L. Marty, A Review of the construction of nano-hybrids for electrochemical biosensing of glucose. *Biosensors*, **9**, 46 (2019).
2. S. Park, H. Boo and T. D. Chung, Electrochemical non-enzymatic glucose sensors. *Anal. Chim. Acta*, **556**, 46 (2006).
3. S. R. Chinnadayyala, K. D. Park and S. Cho, Review—In Vivo and In Vitro microneedle based enzymatic and non-enzymatic continuous glucose monitoring biosensors. *ECS Journal of Solid State Science and Technology*, **7**, Q3159 (2018).
4. X. Niu, X. Li, J. Pan, Y. He, F. Qiu and Y. Yan, Recent advances in non-enzymatic electrochemical glucose sensors based on non-precious transition metal materials: opportunities and challenges. *RSC Advances*, **6**, 84893 (2016).
5. J. Luo, P. Luo, M. Xie, K. Du, B. Zhao, F. Pan, P. Fan, F. Zeng, D. Zhang, Z. Zheng and G. Liang, A new type of glucose biosensor based on surface acoustic wave resonator using Mn-doped ZnO multilayer structure. *Biosens. Bioelectron.*, **49**, 512 (2013).
6. M. Gourzi, A. Rouane, R. Guelaz, M. S. Alavi, M. B. McHugh, M. Nadi and P. Roth, Non-invasive glycaemia blood measurements by electromagnetic sensor: study in static and dynamic blood circulation. *J. Med. Eng. Technol.*, **29**, 22 (2005).
7. C. D. Malchoff, K. Shoukri, J. I. Landau and J. M. Buchert, A novel noninvasive blood glucose monitor. *Diabetes Care*, **25**, 2268 (2002).
8. M. S. Steiner, A. Duerkop and O. S. Wolfbeis, Optical methods for sensing glucose. *Chem. Soc. Rev.*, **40**, 4805 (2011).
9. J. Wang, Electrochemical glucose biosensors. *Chem. Rev.*, **108**, 814 (2008).
10. D.-W. Hwang, S. Lee, M. Seo and T. D. Chung, Recent advances in electrochemical non-enzymatic glucose sensors – A review. *Anal. Chim. Acta*, **1033**, 1 (2018).
11. F. Xie, X. Cao, F. Qu, A. M. Asiri and X. Sun, Cobalt nitride nanowire array as an efficient electrochemical sensor for glucose and H_2O_2 detection. *Sens. Actuators, B*, **255**, 1254 (2018).
12. F. Xie, T. Liu, L. Xie, X. Sun and Y. Luo, Metallic nickel nitride nanosheet: An efficient catalyst electrode for sensitive and selective non-enzymatic glucose sensing. *Sens. Actuators, B*, **255**, 2794 (2018).
13. L. Sinha, S. Pakhira, P. Bhojane, S. Mali, C. K. Hong and P. M. Shirage, Hybridization of Co_3O_4 and α-MnO_2 nanostructures for high-performance nonenzymatic glucose sensing. *ACS Sustainable Chemistry & Engineering*, **6**, 13248 (2018).
14. X. Weina, L. Guanlin, W. Chuanshen, C. Hu and X. Wang, A novel β-MnO_2 micro/nanorod arrays directly grown on flexible carbon fiber fabric for high-performance enzymeless glucose sensing. *Electrochim. Acta*, **225**, 121 (2017).
15. X. Zhu, Y. Ju, J. Chen, D. Liu and H. Liu, Nonenzymatic wearable sensor for electrochemical analysis of perspiration glucose. *ACS sensors*, **3**, 1135 (2018).
16. B. Xue, K. Li, L. Feng, J. Lu and L. Zhang, Graphene wrapped porous Co_3O_4/$NiCo_2O_4$ double-shelled nanocages with enhanced electrocatalytic performance for glucose sensor. *Electrochim. Acta*, **239**, 36 (2017).
17. D. Jiang, Z. Chu, J. Peng, J. Luo, Y. Mao, P. Yang and W. Jin, One-step synthesis of three-dimensional $Co(OH)_2$/rGO nano-flowers as enzyme-mimic

sensors for glucose detection. *Electrochim. Acta*, **270**, 147 (2018).

18. H. Xu, C. Xia, S. Wang, F. Han, M. K. Akbari, Z. Hai and S. Zhuiykov, Electrochemical non-enzymatic glucose sensor based on hierarchical 3D Co_3O_4/Ni heterostructure electrode for pushing sensitivity boundary to a new limit. *Sens. Actuators, B*, **267**, 93 (2018).

19. L. Jia, X. Wei, L. Lv, X. Zhang, X. Duan, Y. Xu, K. Liu and J. Wang, Electrodeposition of hydroxyapatite on nickel foam and further modification with conductive polyaniline for non-enzymatic glucose sensing. *Electrochim. Acta*, **280**, 315 (2018).

20. J. Lv, C. Kong, Y. Xu, Z. Yang, X. Zhang, S. Yang, G. Meng, J. Bi, J. Li and S. Yang, Facile synthesis of novel CuO/Cu_2O nanosheets on copper foil for high sensitive nonenzymatic glucose biosensor. *Sens. Actuators, B*, **248**, 630 (2017).

21. Y. Mao, Z. Mei, L. Liang, B. Zhou and Y. Tian, Robust and magnetically recoverable dual-sensor particles: Real-time monitoring of glucose and dissolved oxygen. *Sens. Actuators, B*, **262**, 371 (2018).

22. Y. Li, X. Niu, J. Tang, M. Lan and H. Zhao, A comparative study of nonenzymatic electrochemical glucose sensors based on Pt-Pd nanotube and nanowire arrays. *Electrochim. Acta*, **130**, 1 (2014).

23. G. Zang, W. Hao, X. Li, S. Huang, J. Gan, Z. Luo and Y. Zhang, Copper nanowires-MOFs-graphene oxide hybrid nanocomposite targeting glucose electro-oxidation in neutral medium. *Electrochim. Acta*, **277**, 176 (2018).

24. Q. Dong, H. Ryu and Y. Lei, Metal oxide based non-enzymatic electrochemical sensors for glucose detection. *Electrochimica Acta*, **370**, (2021).

25. [25] H. Dai, M. Lin, N. Wang, F. Xu, D. Wang and H. Ma, Nickel-foam-wupported Co_3O_4 nanosheets/PPy nanowire heterostructure for non-enzymatic glucose sensing. *ChemElectroChem*, **4**, 1135 (2017).

26. M. Li, C. Han, Y. Zhang, X. Bo and L. Guo, Facile synthesis of ultrafine Co_3O_4 nanocrystals embedded carbon matrices with specific skeletal structures as efficient non-enzymatic glucose sensors. *Anal. Chim. Acta*, **861**, 25 (2015).

27. A. Ray, A. Roy, M. Ghosh, J. Alberto Ramos-Ramón, S. Saha, U. Pal, S. K. Bhattacharya and S. Das, Study on charge storage mechanism in working electrodes fabricated by sol-gel derived spinel $NiMn_2O_4$ nanoparticles for supercapacitor application. *Appl. Surf. Sci.*, **463**, 513 (2019).

28. J. Xu, Y. Sun, M. Lu, L. Wang, J. Zhang, J. Qian and E. J. Kim, Fabrication of porous Mn_2O_3 microsheet arrays on nickel foam as high–rate electrodes for supercapacitors. *J. Alloys Compd.*, **717**, 108 (2017).

29. S. Nagamuthu, S. Vijayakumar, S. H. Lee and K. S. Ryu, Hybrid supercapacitor devices based on $MnCo_2O_4$ as the positive electrode and $FeMn_2O_4$ as the negative electrode. *Appl. Surf. Sci.*, **390**, 202 (2016).

30. X. Liu, W. Zang, C. Guan, L. Zhang, Y. Qian, A. M. Elshahawy, D. Zhao, S. J. Pennycook and J. Wang, Ni-doped cobalt–cobalt nitride heterostructure arrays for high-power supercapacitors. *ACS Energy Letters*, 2462 (2018).

31. F. Zhang, C. Yuan, X. Lu, L. Zhang, Q. Che and X. Zhang, Facile growth of mesoporous Co_3O_4 nanowire arrays on Ni foam for high performance electrochemical capacitors. *J. Power Sources*, **203**, 250 (2012).

32. J. Xu, Y. Sun, M. Lu, L. Wang, J. Zhang, J. Qian and X. Liu, Fabrication of hierarchical $MnMoO_4·H_2O@MnO_2$ core-shell nanosheet arrays on nickel foam as an advanced electrode for asymmetric supercapacitors. *Chem. Eng. J.*, **334**, 1466 (2018).

33. T. H. V. Kumar and A. K. Sundramoorthy, Non-enzymatic electrochemical detection of urea on silver nanoparticles anchored nitrogen-doped single-walled carbon nanotube modified electrode. *J. Electrochem. Soc.*, **165**, B3006 (2018).

34. S. Zhang, D. Li, S. Chen, X. Yang, X. Zhao, Q. Zhao, S. Komarnenid and D. Yang, Highly stable supercapacitors with MOF-derived Co_9S_8/carbon electrodes for high rate electrochemical energy storage. *J. Mater. Chem. A*, **5**, 12453 (2017).

35. Y. Pei, M. Hu, X. Tang, W. Huang, Z. Li, S. Chen and Y. Xia, Ultrafast one-pot anodic preparation of Co_3O_4/nanoporous gold composite electrode as an efficient nonenzymatic amperometric sensor for glucose and hydrogen peroxide. *Anal. Chim. Acta*, **1059**, 49 (2019).

36. L. Wang, Y. Zhang, Y. Xie, J. Yu, H. Yang, L. Miao and Y. Song, Three-dimensional macroporous carbon/hierarchical Co_3O_4 nanoclusters for nonenzymatic electrochemical glucose sensor. *Appl. Surf. Sci.*, **402**, 47 (2017).

37. Y. Gao, Q. Yu, Y. Du, M. Yang, L. Gao, S. Rao, Z. Yang, Q. Lan and Z. Yang, Synthesis of Co_3O_4-NiO nano-needles for amperometric sensing of glucose. *J. Electroanal. Chem.*, **838**, 41 (2019).

38. Z. Yang and X. Bai, Synthesis of Au core flower surrounding with sulphur-doped thin Co_3O_4 shell for enhanced nonenzymatic detection of glucose. *Microchem. J.*, **160**, 105601 (2021).

39. S. Cheng, S. DelaCruz, C. Chen, Z. Tang, T. Shi, C. Carraro and R. Maboudian, Hierarchical Co_3O_4/CuO nanorod array supported on carbon cloth for highly sensitive non-enzymatic glucose biosensing. *Sensors & Actuators: B. Chemical*, **298**, 126860 (2019).

40. M. Harry, M. Chowdhury, F. Cummings and C. J. Arendse, Elemental Cu doped Co_3O_4 thin film for highly sensitive non-enzymatic glucose detection. *Sensing and Bio-Sensing Research*, **23**, 100262 (2019).

41. Y. Zhang, Y. Liu, Y. Bai, X. Li and W. Chu, In situ formation of reduced graphene oxide@Co_3O_4-N-doped carbon and its structure-function relationship for glucose sensing. *Appl. Surf. Sci.*, **539**, 148235 (2021).

42. Z. Gao, L. Zhang, C. Ma, Q. Zhou, Y. Tang, Z. Tu, W. Yang, L. Cui and Y. Li, TiO_2 decorated Co_3O_4 acicular nanotube arrays and its application as a non-enzymatic glucose sensor. *Biosens. Bioelectron.*, **80**, 511 (2016).

43. M. Yassina, B. K. Shrestha, R. Ahmad, S. Shrestha, C. H. Park and C. S. Kim, Exfoliated nanosheets of Co_3O_4 webbed with polyaniline nanofibers: A novel composite electrode material for enzymeless glucose sensing application. *J. Ind. Eng. Chem.*, **73**, 106 (2019).

44. N. Alizadeh, A. Salimi and R. Hallaj, Mimicking peroxidase-like activity of Co_3O_4-CeO_2 nanosheets integrated paper-based analytical devices for detection of glucose with smartphone. *Sens. Actuators, B*, **288**, 44 (2019).

45. X. Lin, Y. Wang, M. Zou, T. Lan and Y. Ni, Electrochemical non-enzymatic glucose sensors based on nano-composite of Co_3O_4 and multiwalled carbon nanotube. *Chin. Chem. Lett.*, **30**, 1157 (2019).

46. V. Coyle, A. E. Kandjani, M. Field, P. Hartley, M. Chen, Y. Sabri and S. Bhargava, Co_3O_4 needles on Au honeycomb as a non-invasive electrochemical biosensor for glucose in saliva. *Biosens. Bioelectron.*, **141**, 111479 (2019).

47. J. Xu, F. Li, D. Wang, M. H. Nawaz, Q. An, D. Han and L. Niu, Co_3O_4 nanostructures on flexible carbon cloth for crystal plane effect of nonenzymatic electrocatalysis for glucose. *Biosens. Bioelectron.*, **123**, 25 (2018).